Quart. J. R. Met. Soc. (1986), **112**, pp. 677–691 551.515.41: 551. 558.1

A new convective adjustment scheme. Part I: Observational and theoretical basis

By A. K. BETTS*

West Pawlet, VT 05775, *U.S.A.*

(Received 12 March 1985; revised 28 January 1986)

SUMMARY

A new convective adjustment scheme is proposed, based on the simultaneous relaxation of temperature and moisture fields towards observed quasi-equilibrium thermodynamic structures, with a relaxation time of order two hours. Separate schemes are used for deep and shallow (non-precipitating) convection.

1. INTRODUCTION

Cumulus parametrization started with simple attempts to represent the subgrid-scale effects of convective clouds. Manabe *et al.* (1965) proposed adjustment towards a moist adiabatic structure in the presence of conditional instability, and Kuo (1965, 1974) proposed a simple cloud model to redistribute the heating and moistening effects of precipitating clouds in the presence of grid-scale moisture convergence. The work of Ooyama (1971) and Arakawa and Schubert (1974) initiated a great deal of research attempting to parametrize cloud ensembles using a cloud spectrum and a simple cloud model (see review by Frank (1983)). One of the key objectives of the GATE experiment (Betts 1974) was to study organized deep convection in the tropics to test and develop convective parametrizations for numerical models. GATE diagnostic studies have documented the complexity of tropical mesoscale convection (Houze and Betts 1981): from the importance of mesoscale updraughts and downdraughts as well as convective-scale processes down to the effects of the cloud microphysical processes of freezing, melting and water loading. One might conclude from these phenomenological studies that cloud models of much greater complexity might be needed to parametrize cumulus convection (Frank 1983). Little progress has been made in this direction, however, because it is clearly impossible to attempt to integrate at each grid-point in a global model, a cloud-scale model of much realism.

This paper returns to a simpler approach to parametrization: the primary objective of the proposed parametrization scheme (Betts 1983b) is to ensure that the local vertical temperature and moisture structures in the large-scale model, which in nature are strongly constrained by convection, be realistic. The concept of a quasi-equilibrium between the cloud field and the large-scale forcing (introduced by Betts (1973) for shallow convection and by Arakawa and Schubert (1974) for deep clouds) has been well established, at least on larger space and time scales (Lord and Arakawa 1980; Lord 1982). This means that convective regions have characteristic temperature and moisture structures which can be documented observationally, and used as the basis of a convective adjustment procedure. Betts (1973) and Albrecht *et al.* (1979) modelled shallow convection using this approach. The main limitation of the moist adiabatic convective adjustment suggested by Manabe *et al.* (1965) for deep convection is that the tropical atmosphere does not approach a moist adiabatic equilibrium structure in the presence of deep convection. In the scheme proposed here we shall relax simultaneously the temperature and moisture structures towards observed quasi-equilibrium structures. This ensures that on the grid scale a global model always maintains a realistic vertical temperature and moisture structure in

* Visiting Scientist at ECMWF.

the presence of convection. This sidesteps all the details of how the subgrid-scale cloud and mesoscale processes maintain the quasi-equilibrium structure we observe. To the extent that one can show observationally that different convective regimes have different quasi-equilibrium thermodynamic structures (as a function of wind shear for example), these could be incorporated using different adjustment parameters. However, given our present limited understanding of different convective regimes, we introduce here the simplest scheme to show its usefulness. The shallow convective adjustment is based on the mixing line structure discussed in Betts (1982a, 1985).

We shall use the saturation point formulation of moist thermodynamics (Betts 1982a) to introduce the observational and theoretical basis of the proposed convective adjustment. We then apply the scheme, in part II of this paper (Betts and Miller 1986), to a series of data sets from GATE, BOMEX, ATEX and an arctic air-mass transformation to show the sensitivity of the scheme to different parameters, and develop a parameter set suitable for both shallow and deep convection in a global model. Part III (in preparation) will show the impact of the scheme on global forecasts.

2. Observational basis

Betts (1982a) has given examples of deep and shallow convective equilibrium structures, and Betts (1983a) has discussed equilibrium structure for mixed stratocumulus layers. Here we present a few examples, which inspired the parametrization scheme. We shall present tephigrams showing temperature and saturation point (abbreviated *sp*) which is temperature and pressure (T^*, p^*) at the lifting condensation level. Isopleths of constant virtual equivalent potential temperature (θ_{ESV}), a *moist virtual adiabat*, for cloudy air will be shown for reference (Betts 1983a), together with $\mathcal{P}$, the difference $(p^* - p)$ between air parcel saturation level and pressure level.

(a) *Deep convection*

(i) *Convective soundings over the tropical ocean.* Figure 1 shows an extreme example: the structure of the deep troposphere for the mean typhoon sounding from Frank (1977). The heavy dots and circles are temperature and saturation point (T, *sp*) for the eyewall. They show a temperature structure which parallels a moist virtual adiabat (θ_{ESV}) below 600 mb, and has θ_{ES} increasing above, with a nearly saturated atmosphere ($p^* - p = \mathcal{P} = -15$ mb). The crosses and symbols E are (T, *sp*) inside the eyewall. Here the strong subsidence has produced a very stable thermal structure, but the *sp* structure is very close to the temperature structure of the eyewall: it has been generated by subsidence of air originally saturated at the eyewall temperature (this does not modify *sp*). The mid-tropospheric subsidence within the eye (of this composite) is 60 mb. Thus the temperature structure of the eyewall is confirmed by two independent composites. Even in this extreme case of strong convection in a typhoon, the mean temperature structure is quite far from moist adiabatic, but quite close to the θ_{ESV} isopleth up to the freezing level.

The light dots and symbols 2 are (T, *sp*) at 2° radius from the storm centre. Here the atmosphere is further from saturation, but has a similar though lower temperature structure. At 200 mb the eyewall $\theta_{ES} \sim 361$ K, while at 2° radius $\theta_{ES} \sim 357$ K, with a corresponding change in θ_E at the low levels.

Figure 2 shows the deep tropospheric structure for the wake (Barnes and Sieckman 1984) of GATE (Global Atmospheric Research Program Atlantic Tropical Experiment) convective band composites. These are tropical convective disturbances weaker than the typhoon. They show a very similar profile to Fig. 1, with an initial decrease of θ_{ES} close to a θ_{ESV} isopleth and then an increase above 600 mb (which is close to the freezing

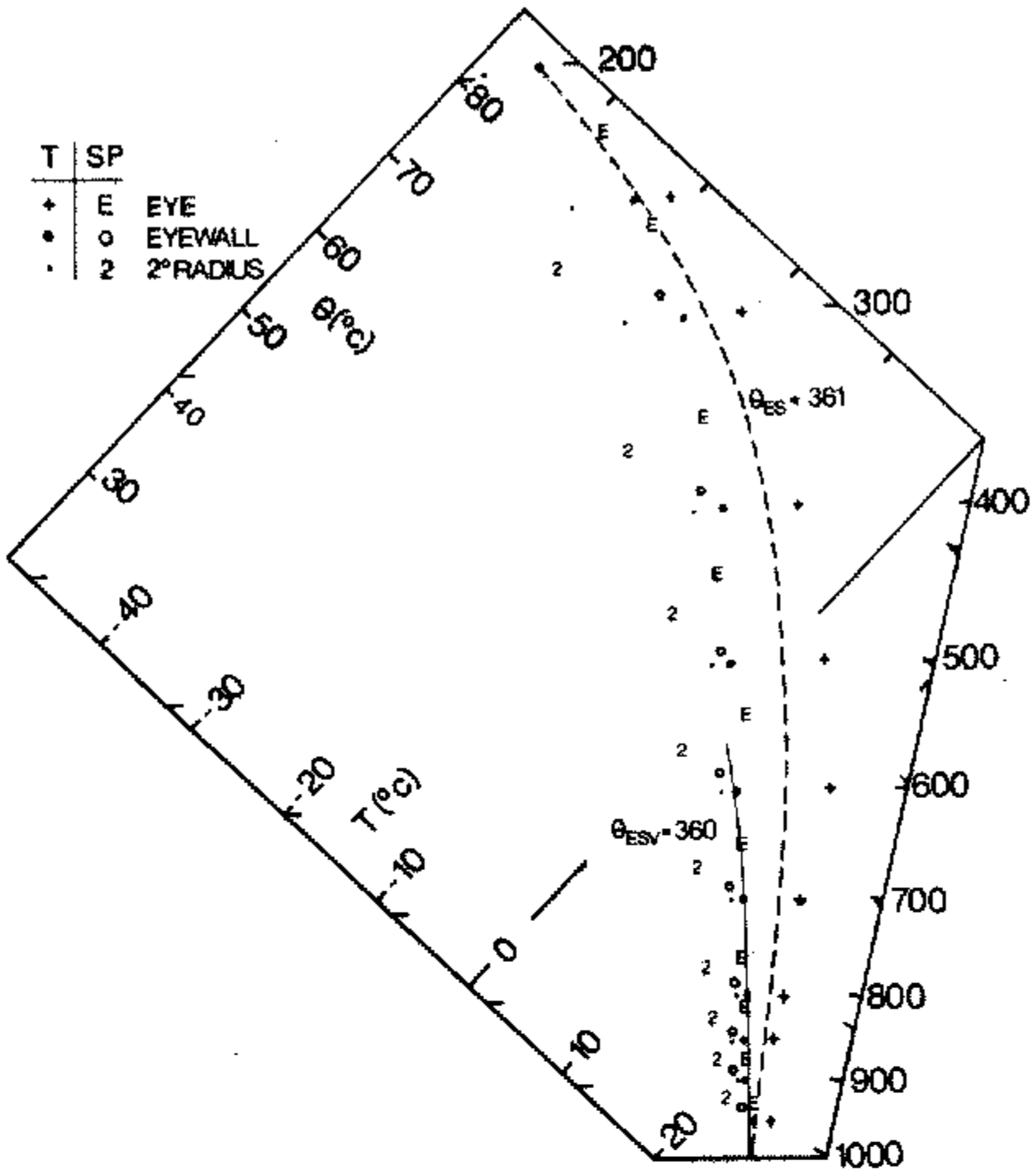

Fig. 1. Composite typhoon sounding inside the eye, the eyewall and 2° radius (Frank 1977), showing T and sp structure.

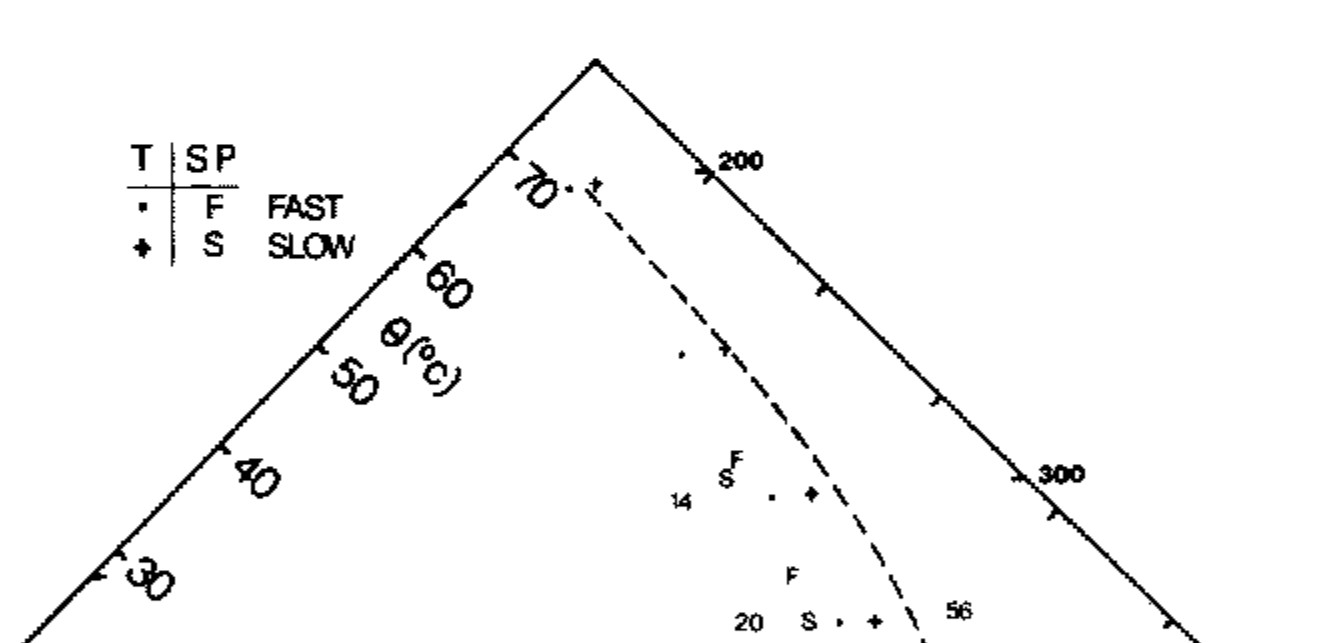

Fig. 2. Composite wake soundings for GATE slow and fast moving lines (Barnes and Sieckman 1984) showing T, sp and $|\mathcal{P}|$ values.

level). The dots and letters F denote the (T, sp) of fast-moving lines (Barnes and Sieckman 1984) and the crosses and letters S denote (T, sp) for slow-moving lines. They show some thermodynamic differences. The $\mathscr{P}$ values for each p level are shown (fast moving on left, slow on right). For reference, $\mathscr{P} = -30$ mb corresponds to a relative humidity of 85% at 800 mb, 75% at 500 mb and 32% at 200 mb at tropical temperatures. The fast-moving line wake has a drier lower troposphere (as a result of stronger downdraughts). Its 600 mb temperature is lower, probably as a response to the falling θ_E in low levels. It is nearly saturated in the upper troposphere corresponding to extensive anvil clouds.

The slow-moving line wake shows the reverse, with a moister lower tropospheric structure and θ_{ES} to 600 mb more closely aligned along a θ_{ESV} isopleth. It, however, is drier in the upper troposphere. These thermodynamic differences are associated with distinct dynamic features in the wind profile: the fast-moving lines have strong shear between the surface and 650 mb (Barnes and Sieckman 1984).

(ii) *Convective equilibrium over land.* Figures 3 and 4 show examples of average soundings on days of major convective episodes over land (Venezuelan International Meteorological and Hydrological Experiment (VIMHEX) in 1972). The small dots are the temperature structure and the circles the corresponding *sp*s. The low-level temperature structures closely parallel a θ_{ESV} isopleth to the freezing level (near 600 mb) and then show an increase of θ_{ES} above. This structure is typical of deep convection in the tropics and may be regarded as more representative of deep convective equilibrium than, say, a moist adiabatic temperature structure. These days do not have fast-moving mesosystems.

(iii) *Deep convective equilibrium structure*: *parametric philosophy*. Most tropical cumulonimbus have small vertical velocities ($\sim 10\,\mathrm{m\,s^{-1}}$) (Zipser and LeMone 1980),

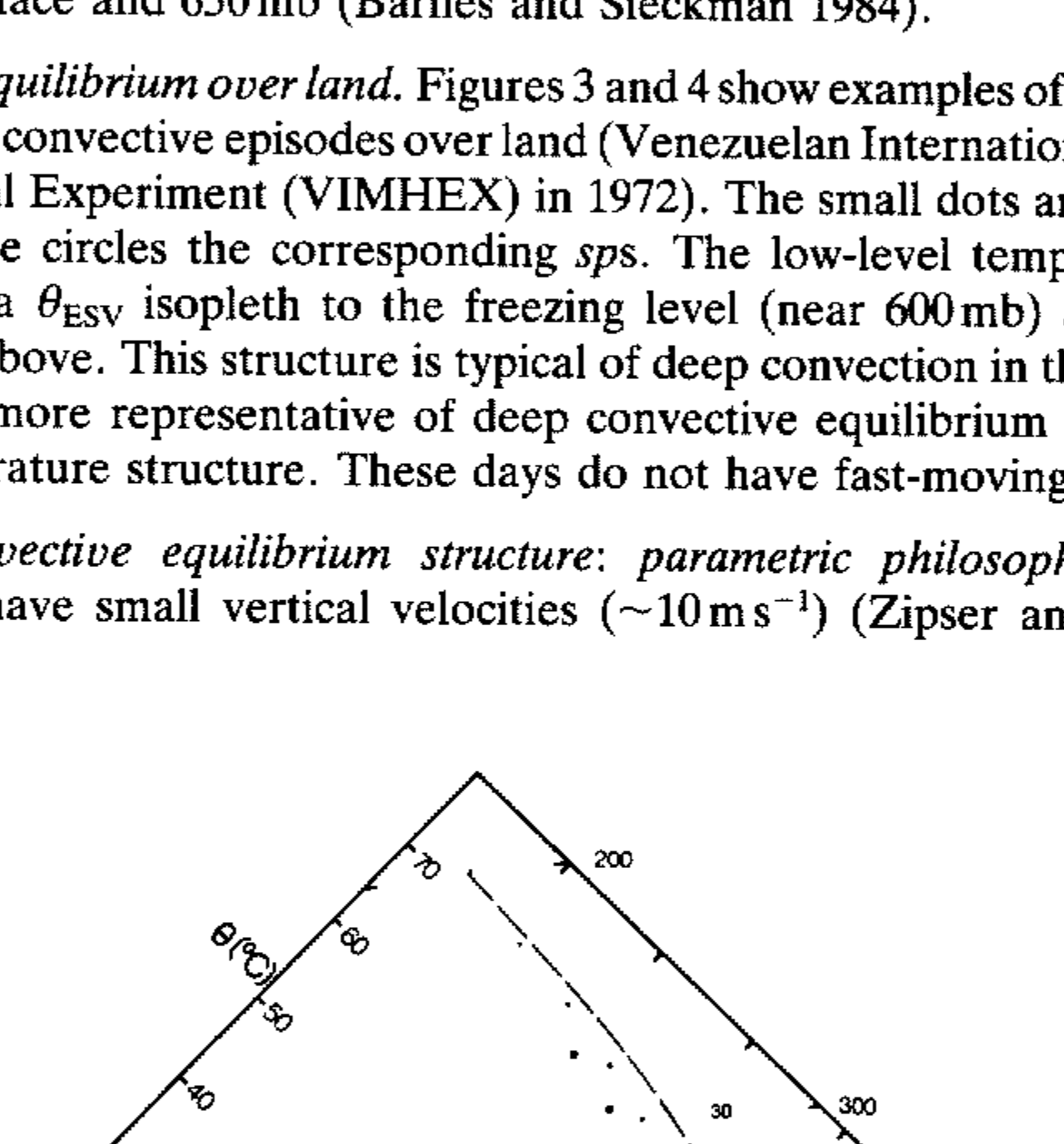

Fig. 3. Composite soundings for 2 September 1972 showing T and sp structure (6 soundings).

and must therefore have correspondingly small mean buoyancy excesses (~0·3 K). Traditionally it has been assumed that temperatures on the moist adiabat are representative of parcel buoyancy for unmixed parcels, but this gives estimates for convective available potential energy far in excess of observed kinetic energies. The moist virtual adiabat (constant θ_{ESV}) which allows for the buoyancy correction for cloud water, has a slope ($d\theta/dz$) only 0·9 times that of the moist adiabat: a marked reduction in buoyancy in the low levels (Betts 1982a). The tendency of deep convective temperature soundings to approach this slope from cloud base to the freezing level (Figs. 1–4) suggests that it is θ_{ESV} rather than θ_{ES} (the moist adiabat) that is the critical reference process in the low troposphere. In physical terms the atmosphere remains slightly unstable to a moist virtual adiabat so that air rising in vigorous cumulus towers remains buoyant until its cloud water is converted to precipitation-size particles.

Closer inspection shows that there may be some observable differences between dynamically different convective systems. All (even the nearly saturated hurricane eyewall convection) show a marked decrease of θ_{ES} below 600 mb, which is the approximate freezing level for this set of tropical data. The temperature structure approximates a θ_{ESV} adiabat suggesting that the lifting of cloud water is a significant density correction in active convective cells in the first few hundred millibars above cloud base. The fast-moving storm composite (Fig. 2) shows a more unstable θ_{ES} structure and correspondingly a drier low-level sp and $\mathcal{P}$ structure associated with stronger unsaturated downdraughts. Perhaps the rapid fall of low-level θ_E prevents a close approach to mid-level thermal equilibrium (see also below).

Around the freezing level, both θ_{ES} and the sp profile show a marked stabilization with a steady increase of both in the upper troposphere toward the θ_{ES} adiabat through

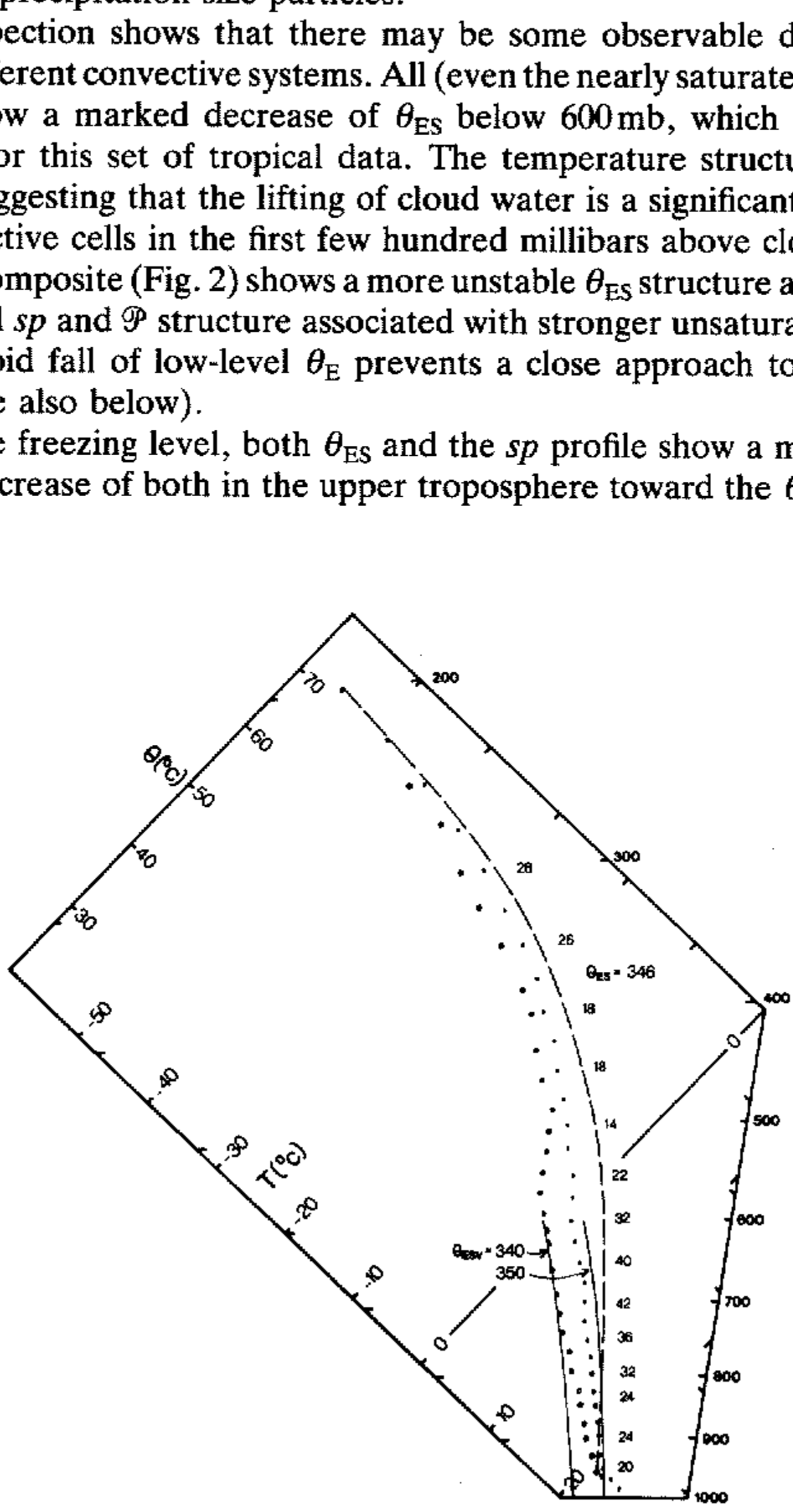

Fig. 4. As Fig. 3 for 9 August 1972 (7 soundings).

a low-level *sp*. This stable structure is probably associated both with freezing and the fallout of precipitation. Both increase cloud parcel buoyancy and we would expect this increase to be reflected in the mean sounding structure if the convection is not far from buoyancy equilibrium with the environment. This suggests also that the sounding minima in θ_{ES} just below the freezing level probably reflect not only the buoyancy correction due to the lifting of cloud water in active cells discussed above, but also the melting of falling precipitation.

The actual computation of cloud parcel buoyancy allowing for fallout and partial freezing would require an elaborate cloud model. We shall adopt a different strategy for parametric purposes. If we assume that quasi-equilibrium means that cloud–environment buoyancy differences become small in regions of active deep convection, then the environmental profile will reflect the cloud-scale processes which alter cloud–parcel buoyancy. We can then use the observed thermodynamic structure as the basis for a parametric adjustment procedure. This seems preferable to attempting to generate in a numerical simulation a realistic quasi-equilibrium structure by the use of cloud models (whether simple or complex).

Our present scheme does not attempt to parametrize the small differences in θ_{ES} structure seen in Figs. 1–4 (although these probably reflect different convective dynamics). Instead the parametric model for deep convection simply constrains θ_{ES} to have a minimum near the freezing level, by using the moist virtual adiabat (θ_{ESV}) as a reference process in the lower troposphere. This is clearly a better adiabat than the moist adiabat (θ_{ES}). An additional gradient parameter (see Eq. (15)) will be tuned using a GATE wave data set.

The $\mathcal{P}$ structure (related to subsaturation) shows more variability related to important physical processes. Fast-moving storms (Fig. 2) with stronger downdraughts have $\mathcal{P} \sim -60$ mb in the low levels (related to a downdraught evaporation pressure scale, Betts (1982b)) compared with $\mathcal{P} \sim -30$ mb in the low levels for the GATE slow-moving lines and the VIMHEX August 9 and September 2 cases (Figs. 2, 3 and 4). Upper-level values of $\mathcal{P}$ are variable in the -20 to -40 mb range: the smaller values (-20 mb) correspond to layers closer to saturation, and presumably to the generation of more extensive cloud layers at outflow levels. However, since we do not have a good understanding of the relationship between these differences and large-scale parameters our parametric model will again simply *specify* a reference $\mathcal{P}$ structure, and use the GATE wave data set for sensitivity and tuning studies. This reference structure may be thought of as a threshold for the onset of precipitation (see section 3).

We adjust from below cloud base up to cloud top. A detailed cloud model is not used to find cloud top for the parametric scheme. Instead cloud top is chosen very simply as the parcel equilibrium height found by constructing a moist adiabat through a low-level θ_E.

(*b*) *Shallow cumulus convection: mixing line structure*

Cumulus convection is a moist mixing process between the subcloud layer and drier air aloft, and not surprisingly the thermodynamic structure tends toward a mixing line (Betts, 1982a, 1984, 1985).

(i) *Mixing line structure*. Figure 5 shows the (T, T_D) structure (solid lines) and corresponding *sp*s (open circles) from the surface to 700 mb for a late afternoon convective sounding over land in the tropics. The entire *sp* structure from 980 to 700 mb lies close to the mixing line joining the end-points. There is a patch of cloud near 750 mb and a dry layer above, but these large fluctuations of T and T_D appear only as *sp* fluctuations

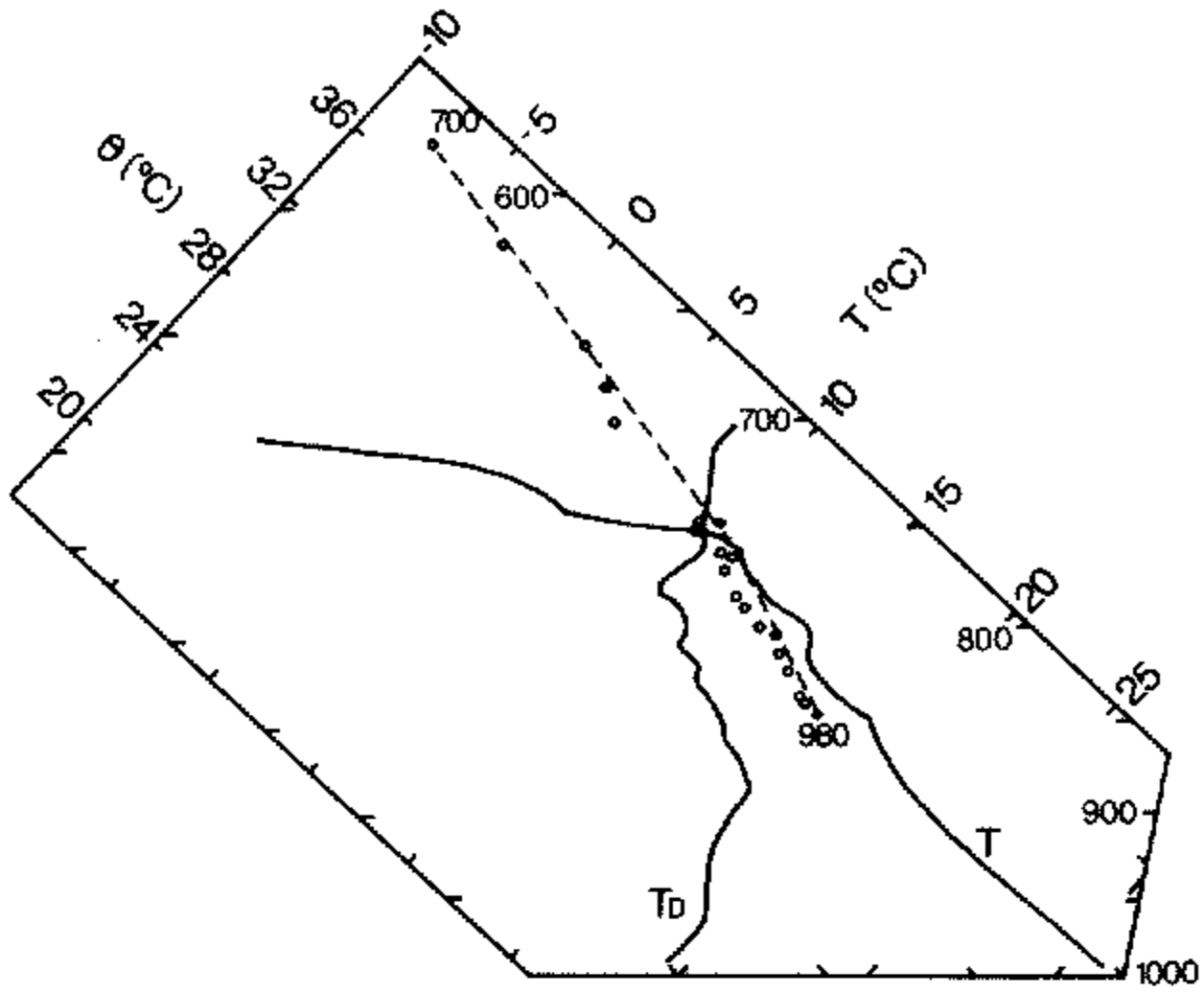

Fig. 5. Late afternoon convective structure, showing *sp*s lying along a mixing line (VIMHEX, Sonde 99, 1972).

up and down the mixing line. The temperature structure in the cloud layer below the stable layer at 700 mb is nearly parallel to the mixing line.

In contrast, air masses that are not convectively mixed show a distinct discontinuity in the *sp* structure. An example is given from GATE in Fig. 6 in which a nearly-moist adiabatic *sp* structure overlies a convectively mixed layer. Three soundings from nearby ships all show the same air-mass transition.

(ii) *Trade cumulus equilibrium.* Figure 7 shows a three-day BOMEX average for the undisturbed trade winds (from Betts 1982a). The dashed line is the mixing line between

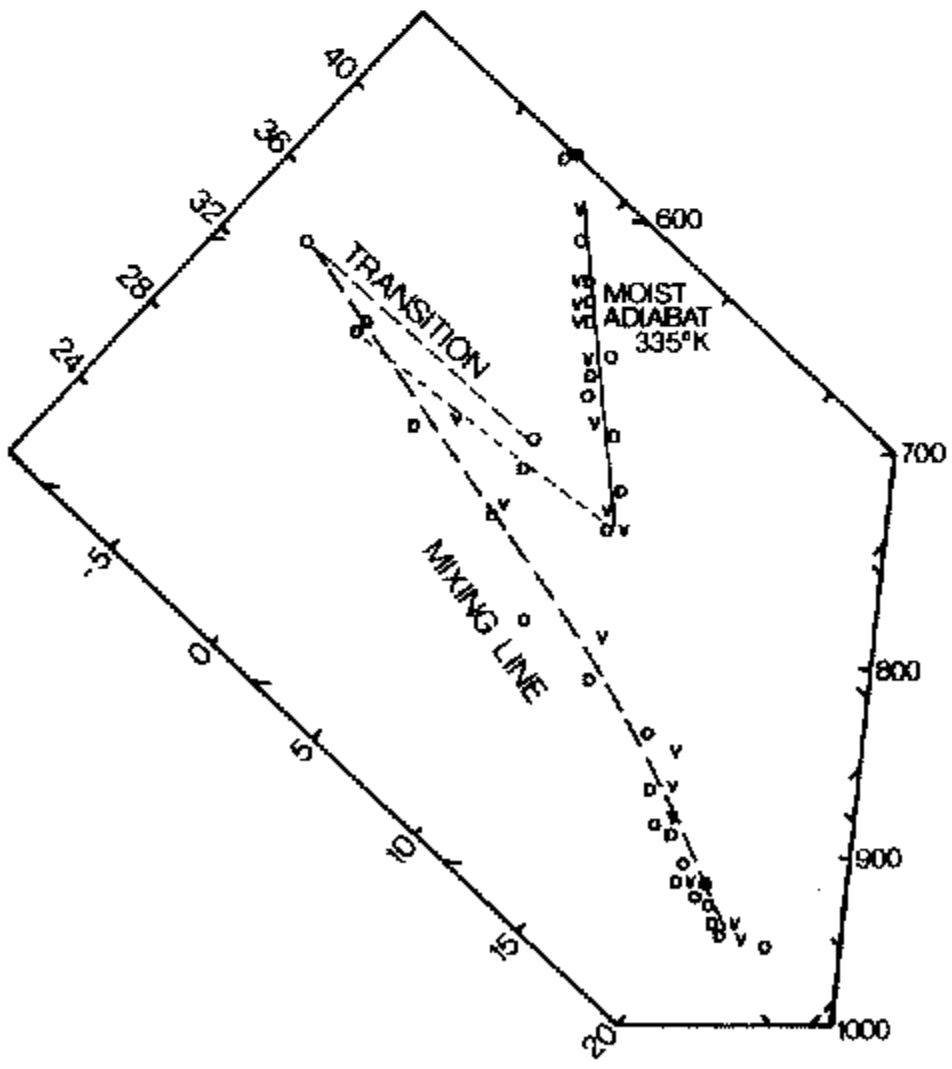

Fig. 6. Soundings at *Oceanographer*, *Vanguard* and *Dallas* on GATE day 258 showing transition between different atmospheric layers.

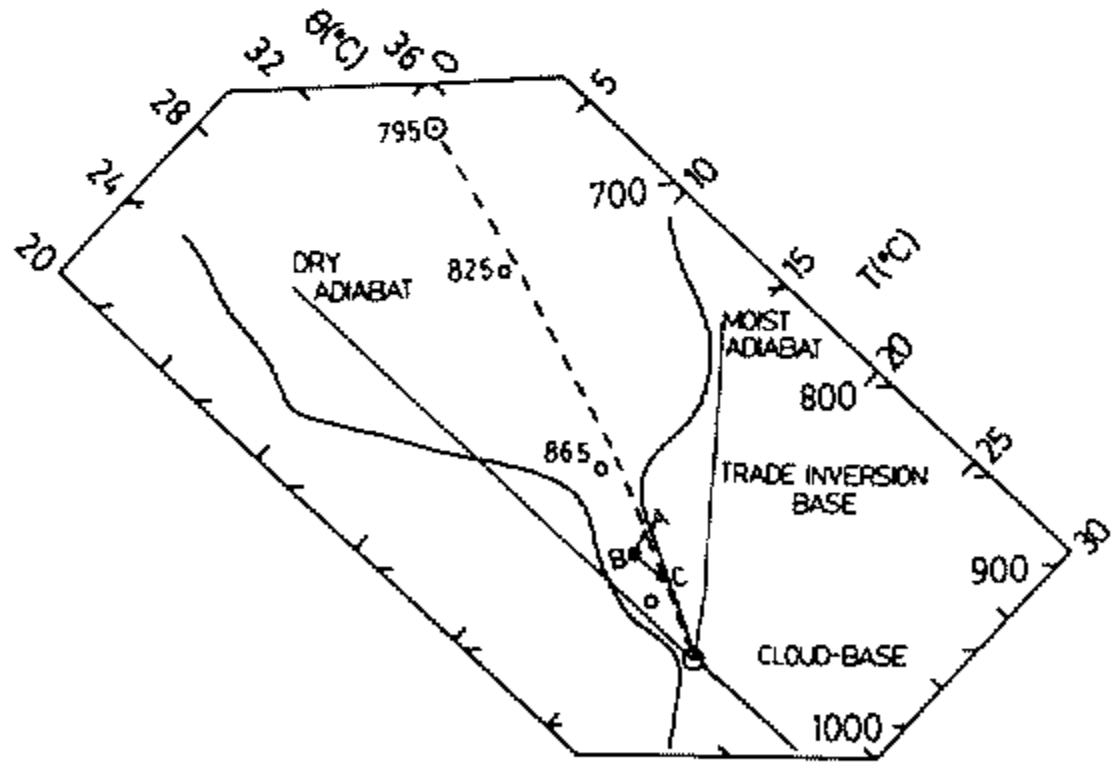

Fig. 7. Three-day sounding for undisturbed trade-wind convection (BOMEX 22–24 June 1969, data kindly supplied by E.M. Rasmusson). Dashed curve is mixing line between inversion top and subcloud air *sp*s. Circles are *sp*s of environment. Vector **AB** denotes generation of environmental *sp* by radiational cooling of air from mixing line.

cloud base air and subsiding air just above the Trade inversion. We note that the lapse rate in the conditionally unstable cumulus layer is very close to the mixing curve (as in Fig. 5). This suggests that the lapse rate in the lower cumulus layer is controlled by the mixing process. The detailed thermodynamic balance involves radiational cooling as well (Betts 1982a).

Figure 8 shows an average for an undisturbed sounding period during the Atlantic Trade Wind Experiment (ATEX) (Augstein *et al.* 1973). The structure is similar to Fig. 7, although the cloud layer lapse rate appears slightly more unstable than the mixing line. However, this average was generated by a special procedure (Augstein *et al.* 1973), designed to sharpen gradients, and may be misleading as a horizontal average. In addition, the profile may be modified by radiative cooling (the cloud cover was >50% for some soundings in the average).

The shallow convection parametrization scheme, though simplified, is based on these examples and others (not shown).

Figure 9 shows a parametric idealization of the coupling of a temperature and dew-point structure of a convective layer to a mixing line. Saturation level pressure $p^*(p)$ locates $T(p)$, $T_D(p)$ on this mixing line. We define a parameter

$$\beta = dp^*/dp \tag{1}$$

and note

$$\partial\theta/\partial p = \beta(\partial\theta/\partial p^*)_M \tag{2a}$$

$$\partial q/\partial p = \beta(\partial q/\partial p^*)_M \tag{2b}$$

where the suffix M denotes the mixing line. Equations (2) relate the mean vertical profiles of θ and q to the gradient of the mixing line. The parameter β represents in some sense the intensity of mixing within and between convective layers.

$\beta = 0$ represents a well-mixed layer: the subcloud layer often approaches this structure. $\beta < 1$ is a layer not as well mixed, in which θ, q converge towards the mixing line. $\beta = 1$ is a partially mixed structure in which the θ, q (or T, T_D) profiles are approximately parallel to the mixing line; while $\beta > 1$ represents the divergence of θ, q from the mixing line that is characteristic of the transition at the top of a convectively mixed layer to the free atmosphere (Fig. 9).

In the basic version of the shallow convection adjustment scheme, we shall specify

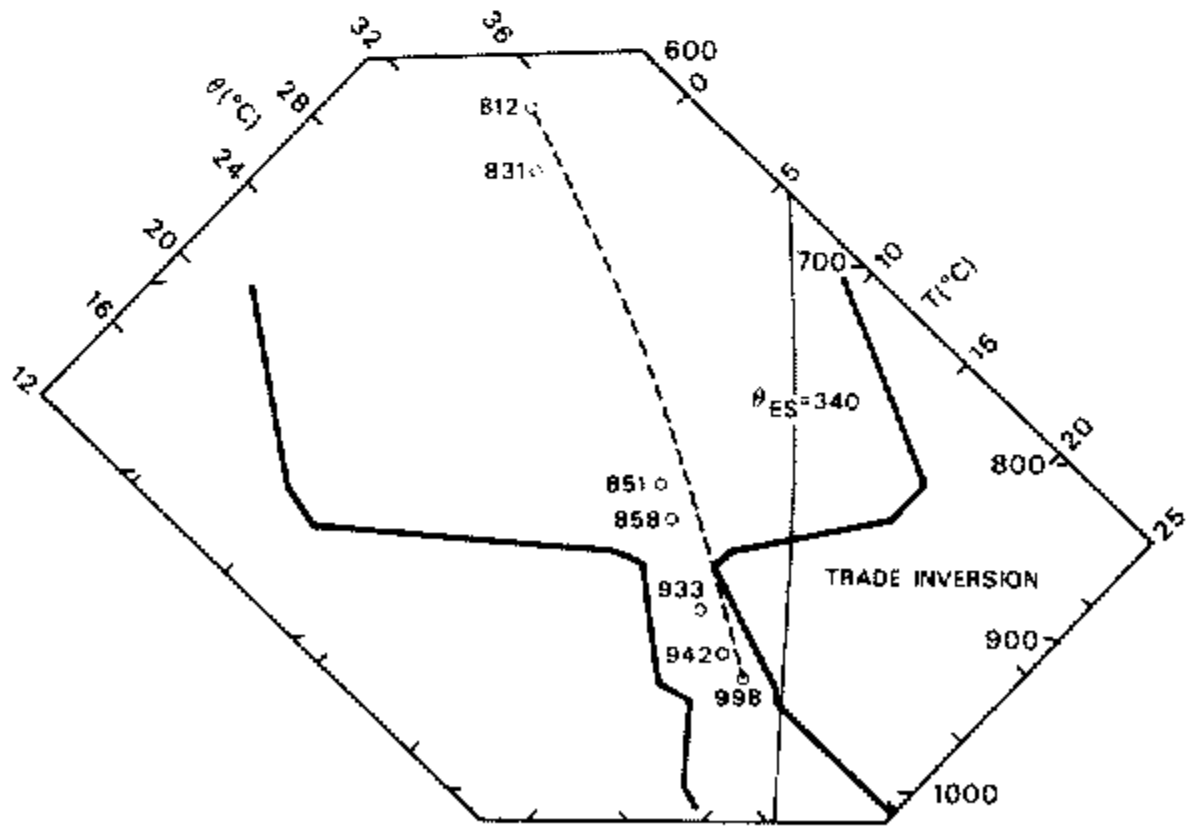

Fig. 8. Undisturbed average sounding (T, T_D) for ATEX (7–12 February 1969). Dashed line is the mixing line between inversion top air and air near the base of the subcloud layer; circles are environmental *sp*s.

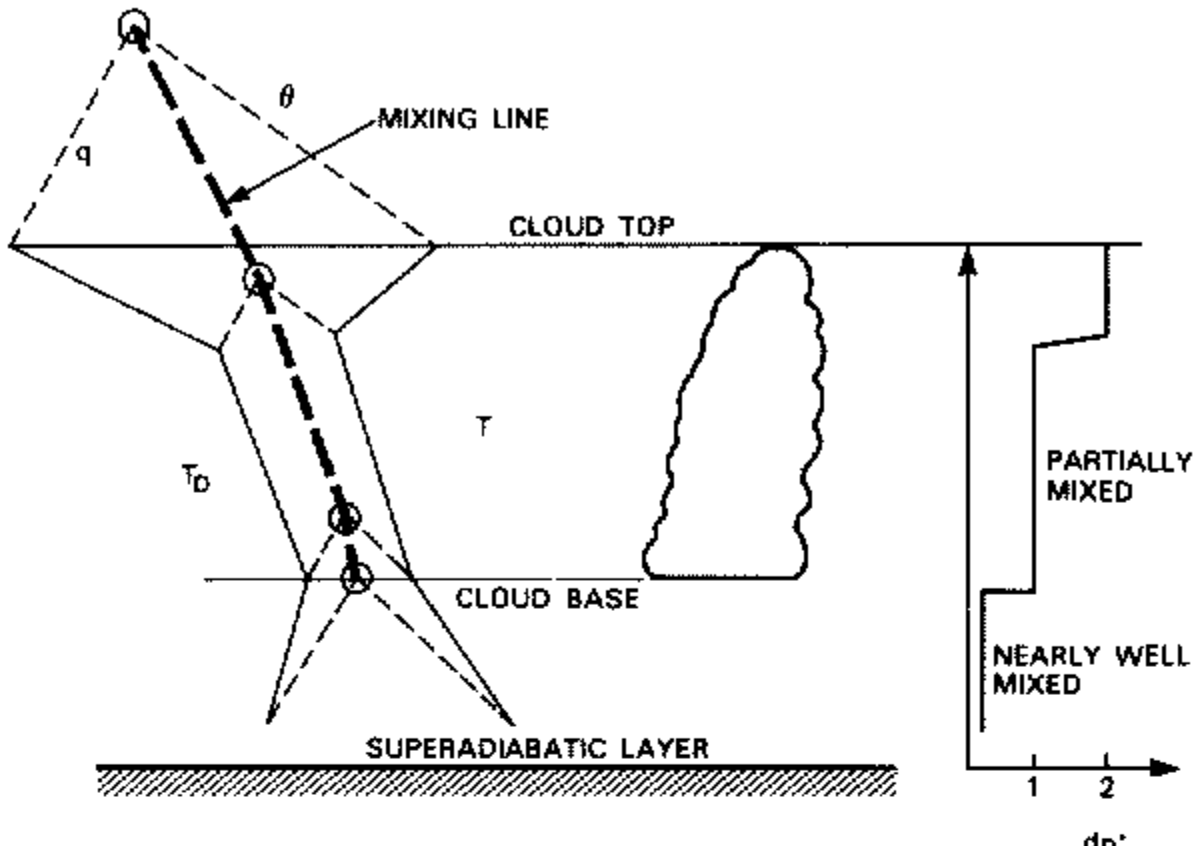

Fig. 9. Idealized cloudy boundary layer thermodynamic structure showing relationship between mixing line, temperature and dew-point soundings and the parameter $\beta = dp^*/dp$ (see text).

$\beta = 1$ from cloud base to cloud top, as a reasonable approximation to Figs. 5, 7 and 8. This means that the lapse rate in the cloud layer is parallel to the mixing line with constant subsaturation parameter $\mathcal{P}$, since $\partial\mathcal{P}/\partial p = \beta - 1 = 0$. The value of $\mathcal{P}$ is not specified but implicitly determined by the two separate integral energy constraints on water vapour and enthalpy, since we assume shallow convection does not precipitate. A linear approximation to the mixing line is computed between low-level air and air from the level above cloud top. Cloud top is found from the intersection with the sounding of a moist adiabat through a low-level θ_E. Although the resulting scheme is somewhat oversimplified, we shall show that it reproduces successfully the main features of shallow convection beneath a capping stable layer (Betts and Miller 1986).

This, like the deep convection adjustment, should be viewed as a preliminary scheme: an approximation to boundary layers with shallow cumulus. For well-mixed stratocumulus layers β has a smaller value close to zero throughout the convective layer because, unlike cumulus layers, the cloud top entrainment instability criterion is not satisfied (Randall 1980; Deardorff 1980). A generalization of the parametric model may well be useful in which β is a function of mixing line slope (Betts 1985) since the mixing line slope governs the cloud top instability (Betts 1982a).

3. Convective adjustment scheme

The scheme is designed to adjust the atmospheric temperature and moisture structure back towards a reference quasi-equilibrium thermodynamic structure in the presence of large-scale radiative and advective processes. Two different reference thermodynamic structures (which are partly specified and partly internally determined) are used for shallow and deep convection, as discussed in section 2.

(a) *Formal structure*

The large-scale thermodynamic tendency equation can be written in terms of $sp(\bar{\mathbf{S}})$, using the vector notation suggested in Betts (1983a), as

$$\partial\bar{\mathbf{S}}/\partial t = -\mathbf{V}\cdot\nabla\bar{\mathbf{S}} - \bar{\omega}\,\partial\bar{\mathbf{S}}/\partial p - g\,\partial\mathbf{N}/\partial p - g\,\partial\mathbf{F}/\partial p \qquad (3)$$

where **N**, **F** are the net radiative and convective fluxes (including the precipitation flux).

The convective flux divergence is parametrized as

$$-g\,\partial \mathbf{F}/\partial p = (\mathbf{R} - \bar{\mathbf{S}})/\tau \tag{4}$$

where **R** is the reference quasi-equilibrium thermodynamic structure and τ is a relaxation or adjustment time representative of the convective or mesoscale processes.

Simplifying the large-scale forcing to the vertical advection, and combining (3) and (4) gives

$$\partial \bar{\mathbf{S}}/\partial t = -\,\overline{\omega}\,\partial \bar{\mathbf{S}}/\partial p + (\mathbf{R} - \bar{\mathbf{S}})/\tau. \tag{5}$$

Near quasi-equilibrium $\partial \bar{\mathbf{S}}/\partial t \approx 0$ so that

$$\mathbf{R} - \bar{\mathbf{S}} \approx \overline{\omega}(\partial \bar{\mathbf{S}}/\partial p)\tau. \tag{6}$$

We shall find that values of τ from 1–2 hours give good results in the presence of realistic forcing. This means that $\mathbf{R} - \bar{\mathbf{S}}$ corresponds to about one hour's forcing by the large-scale fields, including radiation. For deep convection the atmosphere will therefore remain slightly cooler and moister than **R**. Furthermore, for small τ, the atmosphere will approach **R** so that we may substitute $\bar{\mathbf{S}} \approx \mathbf{R}$ in the vertical advection term, giving

$$\mathbf{R} - \bar{\mathbf{S}} \approx \omega\tau\,\partial \mathbf{R}/\partial p \tag{7}$$

from which the convective fluxes can be approximately expressed using (2), as

$$\mathbf{F} = \int \frac{(\mathbf{R} - \bar{\mathbf{S}})}{\tau}\frac{dp}{g} \approx \int \overline{\omega}\frac{\partial \mathbf{R}}{\partial p}\frac{dp}{g}. \tag{8}$$

Equation (8) shows that the structure of the convective fluxes is closely linked to the structure of the specified reference profile **R**. By adjusting towards an observationally realistic thermodynamic structure **R**, we simultaneously constrain the convective fluxes including precipitation to have a structure similar to those derived diagnostically from (3), or its simplified form (8), by the budget method (Yanai *et al.* 1973).

Substituting p^* in (7) gives (suffix R for the reference profile)

$$\mathscr{P}_{\mathrm{R}} - \overline{\mathscr{P}} = p^*_{\mathrm{R}} - \bar{p}^* \approx \omega\tau\, dp^*_{\mathrm{R}}/dp \approx \omega\tau \tag{9}$$

since $1 < dp^*_{\mathrm{R}}/dp < 1{\cdot}1$ for the deep reference profiles which we shall use (see part II). Rearranging gives an approximate value for

$$\overline{\mathscr{P}} \approx \mathscr{P}_{\mathrm{R}} - \omega\tau. \tag{10}$$

Thus while the deep convection scheme is operating, the grid-scale $\overline{\mathscr{P}}$ is shifted by the mean vertical advection $\omega\tau$ mb towards saturation from the specified reference state $\mathscr{P}_{\mathrm{R}}$. Thus, although we specify in the present simple scheme a constant global value of the reference structure $\mathscr{P}_{\mathrm{R}}$, $\overline{\mathscr{P}}$ does have a spatial and temporal variability in the presence of deep convection related to that of $\overline{\omega}$.

The role of convective parametrization in a global model is to produce precipitation before grid-scale saturation is reached both to simulate the real behaviour of atmospheric convection and also to prevent grid-scale instability associated with a saturated conditionally unstable atmosphere. We can see from (10) that if the convection scheme is to prevent grid-scale saturation ($\overline{\mathscr{P}} = 0$), there is a constraint on τ, $\tau < \mathscr{P}_{\mathrm{R}}/\omega_{\max}$, where $\omega_{\max}$ is a typical maximum ω in, say, a major tropical disturbance. With $\mathscr{P}_{\mathrm{R}} \sim -40$ mb, we have found this suggests an upper limit on τ, ~ two hours for the ECMWF T-63 spectral model and ~ one hour for the T-106 model. In part II (Betts and Miller 1986), we shall show that $\tau \sim$ two hours gives the best fit to a GATE wave data set simulated using a single column model. In the global model our preliminary conclusion is that τ

should be set so that the model atmosphere nearly saturates on the grid-scale in major convective disturbances, but this is being investigated further.

(*b*) *Adjustment procedure*

We allow the large-scale advective terms, radiation and surface fluxes, to modify the thermodynamic structure $\overline{\mathbf{S}}$. Cloud top is then found using a moist adiabat through the low-level θ_E. Cloud top height initially distinguishes shallow from deep convection (currently level 11 in the global model; about 780 mb). Different reference profiles are constructed for shallow and deep convection, which satisfy different energy integral constraints. The convective adjustment, $(\mathbf{R} - \mathbf{S})/\tau$, is then applied to the separate temperature and moisture fields as two tendencies (suffix C for convection):

$$(\partial \overline{T}/\partial t)_C = (T_R - \overline{T})/\tau \tag{11}$$

$$(\partial \overline{q}/\partial t)_C = (q_R - \overline{q})/\tau. \tag{12}$$

(*c*) *Reference thermodynamic profiles*

The essence of this convective adjustment scheme is these reference profiles. We initially separate shallow and deep convection by cloud top.

(i) *Shallow convection.* For shallow convection the reference profile $\mathbf{R}_S$ is constructed to satisfy the two separate energy constraints

$$\int_{p_B}^{p_T} c_p(T_R - \overline{T})\, dp = \int_{p_B}^{p_T} L(q_R - \overline{q})\, dp = 0 \tag{13a}$$

so that the condensation (and precipitation) rates are zero, when integrated from cloud base p_B to cloud top p_T. This implies that the shallow convection scheme does not precipitate, but simply redistributes heat and moisture in the vertical.

(ii) *Deep convection.* For deep convection the reference profile $\mathbf{R}_D$ is constructed to satisfy the total enthalpy constraint

$$\int_{p_B}^{p_T} (H_R - \overline{H})\, dp = 0 \tag{13b}$$

where $H = c_pT + Lq$ and p_B, p_T are a cloud base level and cloud top pressure respectively. In the tests discussed in Betts and Miller (1986), p_B is fixed at $\sigma = 0{\cdot}98$. (In subsequent global model tests, the deep convective adjustment is made down to within a few millibars of the surface (one level above the model surface).) The precipitation rate is then given by

$$PR = \int_{p_B}^{p_T} \left(\frac{q_R - \overline{q}}{\tau}\right) \frac{dp}{g} = -\frac{c_p}{L} \int_{p_B}^{p_T} \left(\frac{T_R - \overline{T}}{\tau}\right) \frac{dp}{g}. \tag{14}$$

No liquid water is stored in the present scheme, and the deep convective adjustment is suppressed if it ever gives $PR < 0$.

This scheme handles the *partition* between moistening of the atmosphere and precipitation in a quite different way from Kuo's, which typically specifies a fixed partitioning of the moisture convergence. Given moisture convergence and (say) mean grid-scale upward motion, the model atmosphere moistens with no precipitation until a threshold is reached, qualitatively related to a mean value of $\mathscr{P}_R$, when precipitation

starts. However, the model atmosphere continues to moisten (given steady state forcing) until (10) is satisfied, when the moistening ceases, and the 'converged moisture' is then all precipitated. If the forcing ceases ($\omega \to 0$) then precipitation continues for a while, until the atmosphere has dried out to the reference profile again. We are essentially controlling (through $\mathscr{P}$) the relative humidity of air leaving convective disturbances. In medium- and longer-range integrations of a global model this seems a better way of maintaining the long-term moisture structure of the atmosphere than through constraints on the partition of moisture convergence.

(*d*) *Computation of deep convection reference profile*

(i) *First-guess profile.* The temperature profile has a minimum $\theta_{ES}(M)$ at the freezing level, p_M. The low-level decrease is based on the gradient V of the θ_{ESV} isopleth multiplied by a weighting coefficient, α. The first-guess profile is established using (15) and (16). For $p_B > p > p_M$

$$\theta_{ES} = \theta_{ES}(B) + \alpha V(p - p_B) \tag{15}$$

where

$$V = (\partial \theta_{ES}/\partial p)_{\theta_{ESV}}.$$

For $p_T < p < p_M$

$$\theta_{ES} = \theta_{ES}(M) + \{\theta_{ES}(T) - \theta_{ES}(M)\}(p - p_T)/(p_M - p_T). \tag{16}$$

This is just a linear increase back to the environmental θ_{ES} at cloud top, p_T. Tests using a GATE wave data set (Betts and Miller 1986) showed that $\alpha = 1{\cdot}5$ gave a realistic tropospheric temperature structure. This reference profile in the low troposphere is therefore just slightly unstable to the θ_{ESV} isopleth, and has a gradient (compared to the dry and moist adiabats) of

$$(\partial \theta_{ES}/\partial p)_R \simeq 0{\cdot}15\,(\partial \theta_{ES}/\partial p)_\theta$$

or the equivalent

$$(\partial \theta/\partial p)_R \simeq 0{\cdot}85\,(\partial \theta/\partial p)_{\theta_{ES}}.$$

The moisture profile is found from the temperature profile by specifying a grid-point mean $\mathscr{P} = (p^* - p)$ at three levels, cloud base ($\mathscr{P}_B$), the freezing level ($\mathscr{P}_M$) and cloud top ($\mathscr{P}_T$) with linear gradients between.

For $p_B > p > p_M$, this gives

$$\mathscr{P}(p) = \{(p_B - p)\mathscr{P}_M + (p - p_M)\mathscr{P}_B\}/(p_B - p_M) \tag{17}$$

and for $p_M > p > p_T$

$$\mathscr{P}(p) = \{(p_M - p)\mathscr{P}_T + (p - p_T)\mathscr{P}_M\}/(p_M - p_T). \tag{18}$$

In the present scheme $\mathscr{P}_B$, $\mathscr{P}_M$, $\mathscr{P}_T$ are chosen to be negative (unsaturated), with $|\mathscr{P}|$ a maximum at the freezing level.

(ii) *Energy correction.* $T(p)$ and $q(p)$ are computed from $\theta_{ES}(p)$ and $\mathscr{P}(p)$ and then a correction to the reference profile is made to satisfy Eq. (13b). We find

$$\Delta H = (p_B - p_T)^{-1} \int_{p_B}^{p_T} (H_R^1 - H_{\bar{S}})\, dp \tag{19}$$

where H_R^1 is from the first-guess reference profile and H_S is for the gridpoint thermodynamic structure. A constant correction is applied to the first-guess reference profile, at all levels (except the cloud top level) of

$$\Delta H' = \Delta H(p_B - p_T)/(p_B - p_{T^-}) \tag{20}$$

where p_{T^-} is at the σ level below cloud top. At each level the temperature field is corrected, with $\mathcal{P}$ kept constant, so as to change $H = (c_p T_R + Lq_R)$ by $\Delta H'$. Applying no correction at cloud top means that the adjustment scheme corrects the q field at cloud top (through the first guess) but not the T field. This is necessary in the global model to avoid systematic corrections at levels just below the tropopause. However, it is also consistent with cloud top being near the level of thermal equilibrium. One iteration is made on this energy correction step to ensure the subsequent adjustment conserves energy to high accuracy.

(e) *Computation of shallow convection reference profile*

(i) *First-guess profile.* The slope of the mixing line is computed from the properties of air at the level p_B and the level above cloud top p_{T^+}. This is done by first finding the *sp* on the mixing line corresponding to an equal mixture of air from the levels p_B and p_{T^+}. This level, denoted (1), is then used to give a linearized mixing line slope in the lower troposphere using

$$M = \{\theta_E(1) - \theta_E(B)\}/\{p_{SL}(1) - p_{SL}(B)\} \tag{21}$$

where $p_{SL}(1)$, $p_{SL}(B)$ are the corresponding saturation level pressures. In the 15-layer gridpoint model we use level 14 for p_B to avoid interaction problems with the diffusion scheme which computes the surface fluxes. The first-guess temperature profile is specified as parallel to the mixing line (corresponding to $\beta = 1$ in Fig. 9) by first computing

$$\theta_{ES}(p) = \theta_{ES}(B) + M(p - p_B). \tag{22}$$

$\theta_{ES}(p)$ is inverted to give (T, p) which together with $\mathcal{P}$ (a first-guess independent of p) gives the *sp* and hence specific humidity.

(ii) *Enthalpy and moisture correction.* Shallow convection is specified as non-precipitating so that the vertical integrals of c_pT and Lq are separately conserved (Eq. (13a)). To ensure this, the first-guess T, q are corrected at each level by

$$\Delta T = (p_B - p_T)^{-1} \int_{p_B}^{p_T} (T - T_R)\, dp \tag{23}$$

$$\Delta q = (p_B - p_T)^{-1} \int_{p_B}^{p_T} (q - q_R)\, dp. \tag{24}$$

By making this correction independent of pressure, we preserve (to sufficient accuracy) the slope M of the θ_{ES} profile, and a value of $\mathcal{P}$ independent of pressure. Since we have two constraints, rather than the one (Eq. (19)) for deep convection, it is not necessary to constrain $\mathcal{P}$. Instead, after applying the corrections (23) and (24), the adjustment closely conserves the vertically averaged value of $\mathcal{P}$ through the shallow convective layer.

4. Concluding remarks

Convective adjustment schemes have been proposed for deep and shallow convection. In their present form they are quite simple, but their structure allows for further

development as our understanding of convective equilibrium from observational studies advances. This proposed interaction between the parametric scheme and diagnostic studies is a novel feature, and a shift in philosophy in cumulus parametrization. It is prompted by many observational experiments which have demonstrated the complexity of convective processes in the atmosphere. It seems unlikely that all the details can be simulated in a parametric submodel for cumulus clouds. Indeed this was never the objective of cumulus parametrization in global models. Observational studies have shown, however, the value of the quasi-equilibrium hypothesis on large space- and time-scales, and the usefulness of the mixing line concept in the study of shallow convection. So we have chosen as a basis for this scheme to directly adjust the temperature and moisture structure toward quasi-equilibrium reference profiles, using our observational data base for calibration where necessary. Examples are given in part II (Betts and Miller 1986). This adjustment implicitly determines the vertical transports of heat and moisture by the convective field. So far we have not attempted to include a convective momentum transport in the scheme.

Another novel aspect of the scheme is the relaxation time-scale, τ. This was introduced to simulate the lag between the changing large-scale field and the convective response toward a quasi-equilibrium reference state. Betts and Miller (1986) show the effect of changing τ on the simulation of a GATE wave data set, and a later paper will show its impact in the global model. However, we know from diagnostic studies (Houze and Betts 1981) of tropical cloud clusters, that the evolution on the mesoscale is important to their structure and evolution. Whether the time-scale τ should include in some way a dependence on mesoscale processes is an area needing further work.

Acknowledgments

This work was supported by ECMWF while the author was a visitor, and by the National Science Foundation under grant ATM-8403333.

References

Arakawa, A. and Schubert, W. H. 1974 Interaction of a cumulus cloud ensemble with the large-scale environment: Part I. *J. Atmos. Sci.*, **31,** 674–701

Albrecht, B. A., Betts, A. K. Schubert, W. H. and Cox, S. K. 1979 A model of the thermodynamic structure of the trade-wind boundary layer: Part I. Theoretical formulation and sensitivity tests. *ibid.*, **36,** 73–89

Augstein, E., Riehl, H., Ostopoff, F. and Wagner, V. 1973 Mass and energy transports in an undisturbed Atlantic trade-wind flow. *Mon. Wea. Rev.*, **101,** 101–111

Barnes, G. M. and Sieckman, K. 1984 The environment of fast and slow tropical mesoscale convective cloud lines. *ibid.*, **112,** 1782–1794

Betts, A. K. 1973 Non-precipitating cumulus convection and its parameterization. *Quart. J. R. Met. Soc.*, **99,** 178–196

1974 The scientific basis and objectives of the US convection subprogram for the GATE. *Bull. Amer. Met. Soc.*, **55,** 304–313

1982a Saturation point analysis of moist convective overturning. *J. Atmos. Sci.*, **39,** 1484–1505

1982b Cloud thermodynamic models in saturation point coordinates. *ibid.*, **39,** 2182–2191

1983a Thermodynamics of mixed stratocumulus layers: saturation point budgets. *ibid.*, **40,** 2655–2670

1983b 'Atmospheric convective structure and a convection scheme based on saturation point adjustment'. Workshop on convection in large-scale models, 28 Nov. to 1 Dec. ECMWF.

	1984	Boundary layer thermodynamics of a high-plains severe storm. *Mon. Wea. Rev.*, **112,** 2199–2211
	1985	Mixing line analysis of clouds and cloudy boundary layers. *J. Atmos. Sci.*, **42,** 2751–2763
Betts, A. K. and Miller, M. J.	1986	A new convective adjustment scheme. Part II: Single column tests using GATE wave, BOMEX, ATEX and arctic air-mass data sets. *Quart. J. R. Met. Soc.*, **112,** 693–709
Deardorff, J. W.	1980	Cloud-top entrainment instability. *J. Atmos. Sci.*, **37,** 131–147
Frank, W. M.	1977	The structure and energetics of the tropical cyclone. Part I: Storm structure. *Mon. Wea. Rev.*, **105,** 1119–1135
	1983	The cumulus parameterization problem. *ibid.*, **111,** 1859–1871
Houze, R. A. and Betts, A. K.	1981	Convection in GATE. *Rev. Geophys. and Space Phys.*, **19,** 541–576
Kuo, H. L.	1965	On formation and intensification of tropical cyclones through latent heat release by cumulus convection. *J. Atmos. Sci.*, **22,** 40–63
	1974	Further studies of the parameterization of the influence of cumulus convection on large-scale flow. *ibid.*, **31,** 1232–1240
Lord, S. J.	1982	Interaction of a cumulus cloud ensemble with the large-scale environment. Part III: Semi-prognostic test of the Arakawa–Schubert cumulus parameterization. *ibid.*, **39,** 88–103
Lord, S. J. and Arakawa, A.	1980	Interaction of a cumulus cloud ensemble with the large-scale environment. Part II. *ibid.*, **37,** 2677–2692
Manabe, S., Smagorinsky, J. and Strickler, R. F.	1965	Simulated climatology of a general circulation model with a hydrologic cycle. *Mon. Wea. Rev.*, **93,** 769–798
Ooyama, K.	1971	A theory of parameterisation of cumulus convection. *J. Meteor. Soc. Japan*, **49,** 744–756
Randall, D. A.	1980	Conditional instability of the first kind upside-down. *J. Atmos. Sci.*, **37,** 125–130
Yanai, M., Esbensen, S. and Chou, J.	1973	Determination of the bulk properties of tropical cloud clusters from large-scale heat and moisture budgets. *ibid.*, **30,** 611–627
Zipser, E. J. and LeMone, M. A.	1980	Cumulonimbus vertical velocity events in GATE. Part II: Synthesis and model core structure. *ibid.*, **37,** 2458–2469